Three different routes from the directed Ising to the directed percolation class

Su-Chan Park

Institut für Theoretische Physik, Universität zu Köln, Zülpicher Strasse 77, 50937 Köln, Germany

Hyunggyu Park

School of Physics, Korea Institute for Advanced Study, Seoul 130-722, Korea
(Received 23 July 2008; published 29 October 2008)

The scaling nature of absorbing critical phenomena is well understood for the directed percolation (DP) and the directed Ising (DI) systems. However, a full analysis of the crossover behavior is still lacking, which is of our interest in this study. In one dimension, we find three different routes from the DI to the DP classes by introducing a symmetry-breaking field (SB), breaking a modulo 2 conservation (CB), or making channels connecting two equivalent absorbing states (CC). Each route can be characterized by a crossover exponent, which is found numerically as $\phi = 2.1 \pm 0.1$ (SB), 4.6 ± 0.2 (CB), and 2.9 ± 0.1 (CC), respectively. The difference between the SB and CB crossover can be understood easily in the domain wall language, while the CC crossover involves an additional critical singularity in the auxiliary field density with the memory effect to identify itself independent.

I. INTRODUCTION

Critical behavior of absorbing phase transitions can be categorized by universality classes [1]. The most well-known example is the directed percolation (DP) class which may be (loosely) defined by a classification scheme known as the "DP conjecture" [2–4]. The conjecture states that models exhibiting a continuous transition into a *single* absorbing state should belong to the DP class unless symmetry or conservation is involved. The DP conjecture may be extended to include some models with multiple absorbing states without any clear-cut symmetry among them [5–7]. For example, the pair contact process [8] allows infinitely many absorbing states but exhibits the DP-type critical behavior at least in its stationary property [9]. However, the controversy over the pair contact process with diffusion (PCPD) in one dimension (whether the PCPD belongs to the DP class or not) has not subsided as yet even with extensive efforts both numerically and analytically [10–16]. Therefore a full understanding for categorizing the DP class is still incomplete.

Nevertheless, the DP conjecture is useful enough to trigger a search for a non-DP universality class. One can find several universality classes in Ref. [1] which do not meet the constraint of the DP conjecture. Among them, we are interested in the system with two equivalent absorbing states (or, in general, two equivalent groups of absorbing states) [17–21]. The Ising-type Z_2 symmetry between two absorbing states, which is sometimes manifest as a modulo 2 conservation of domain walls in one dimension, renders the system to exhibit a non-DP critical behavior. This universality class has several names, such as the parity conserving [17,18]; the directed Ising (DI) [19,22,23]; which will be used to refer to this class in this paper, the generalized voter class [24]; and so on. In higher dimensions, all these classes become distinct.

The Ising symmetry (or the modulo 2 conservation) *per se* is not enough to force the DI critical behavior. It requires an infinite dynamic barrier between two equivalent (groups of) absorbing states [5,22], which is analogous to the free energy barrier between two ordered states in the equilibrium Ising model. A state near one absorbing state cannot evolve into the other absorbing state within a finite number of successive local changes. In other words, a domain wall (frustration) in a configuration generated by pasting two absorbing states cannot disappear by itself, so the system never becomes absorbing with a single frustration [5,11].

As an example without this additional feature, consider a one-dimensional system of diffusing particles with pair annihilation ($2A \to \emptyset$) and branching of two particles by a triplet ($3A \to 5A$). We may map this particle model onto the ferromagnetic Ising spin model by interpreting a particle as a domain wall of the Ising system as follows:

$$A\emptyset \leftrightarrow \emptyset A \mapsto \uparrow\downarrow\downarrow \leftrightarrow \uparrow\uparrow\downarrow,$$

$$AA \to \emptyset\emptyset \mapsto \uparrow\downarrow\uparrow \to \uparrow\uparrow\uparrow,$$

$$\emptyset AAA\emptyset \to AAAAA \mapsto \downarrow\downarrow\uparrow\downarrow\uparrow\uparrow \to \downarrow\uparrow\downarrow\uparrow\downarrow\uparrow, \quad (1)$$

where A ($\emptyset$) stands for a particle (vacancy) and $\uparrow$ ($\downarrow$) represents an up (down) spin. Clearly the number of domain walls is conserved modulo 2 and there are two absorbing states in the spin system (all spins are up or down) which are equivalent. However, the states with only one (diffusing) particle are also absorbing in the particle model. In the spin language, these extra absorbing states can be obtained by connecting two equivalent absorbing states (for example, $\cdots\uparrow\uparrow\uparrow\downarrow\downarrow\downarrow\cdots$), which violate the infinite dynamic barrier requirement for the DI universality class mentioned above [5,22]. It is numerically shown that this system shares the critical behavior with the DP but not the DI [11,25], while a similar system with $2A \to \emptyset$ and $2A \to 4A$ belongs to the PCPD class [26]. It is claimed that long-term memory plays a crucial role in differentiating these two universality classes [12].

According to the above criterion for the DI class, one can conceive three possible (independent) routes along which the DI critical behavior crosses over to the DP in one dimension.

Introducing a symmetry-breaking field (SB) [22,27–31], allowing dynamics which breaks the modulo 2 conservation (CB) [32,33], or making channels connecting two equivalent absorbing states (CC) [5,7] drives the system into the DP class. These three routes bring about different characteristics in the absorbing states. The SB route maintains the absorbing states but breaks the probabilistic balance between them. The CB route (for example, by adding $A \to \emptyset$ or $2A$) invalidates the mapping between the spin and the particle model, and ends up with only one absorbing state (vacuum). The CC route is accompanied by additional (infinitely many) absorbing states connecting two equivalent absorbing states with both the symmetry and the mapping sustained.

The crossover behavior from one fixed point to another does not reflect the properties of both fixed points, in general. Rather, strictly speaking, it is related to one fixed point and its crossover operator, which forces the system to cross over to the other fixed point [15,34,35]. In many cases, the crossover route is unique between two fixed points; so is the crossover operator, which leads to one unique crossover exponent between two universality classes. In our case, the crossover operators for three different routes seem to be qualitatively different from each other. To quantify this difference and confirm the independence of the three crossover routes, we measure the crossover exponents governing the crossover behavior by numerical simulations.

In Sec. II, one-dimensional models are introduced belonging to the DI class. In Sec. III, numerical results for the crossover exponents along the three different routes are reported. In Sec. IV, we discuss the underlying fundamental difference in the three crossover operators, in particular, focusing on the origin of the CC crossover distinct from the CB crossover. Finally, a brief summary is given in Sec. V.

II. DI MODELS

We choose two DI models for studying crossover from the DI class to the DP class: branching annihilating walks with two offspring (BAW2) [18,21] and the interacting monomer model (IM), which is a simplified version of the interacting monomer-monomer model [7]. We study the macroscopic absorbing phase transitions [25] inherent in the models. The suitable order parameters will be defined when we explain each model in detail. For convenience, the order parameter will be denoted by ρ throughout the paper. We only study one-dimensional lattice systems with periodic boundary conditions.

For the simulation of the BAW2, we take the dynamic branching rule of Ref. [32]. The simulation algorithm is detailed as follows: At first, we choose a particle residing at a lattice point randomly among N_t particles present at time t. It may hop to a randomly chosen nearest neighbor site with probability p. If the target site is already occupied, two particles are removed immediately. With probability $(1-p)$, this selected particle branches two particles along one of two directions. If an offspring is created on a site already occupied, both particles annihilate immediately. After the above steps, time increases by $1/N_t$. Since the absorbing state is the vacuum, the order parameter ρ is the particle density. At
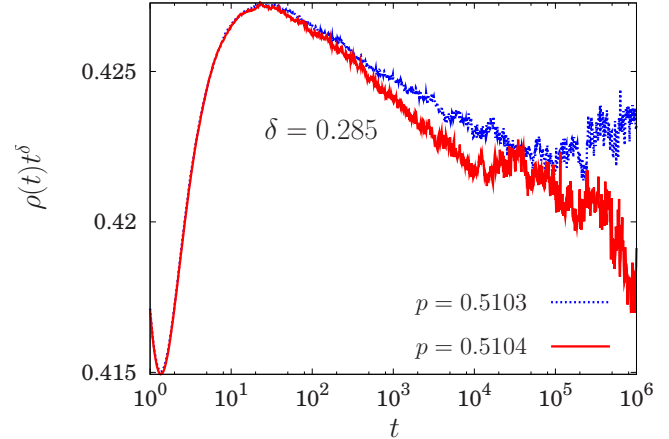

FIG. 1. (Color online) Semilogarithmic plot of $\rho(t)t^\delta$ vs t near criticality for the BAW2. The critical point is found to be $p_c = 0.510\,35(5)$ with the figure in the parentheses as uncertainty of the last digit.

criticality, the density is expected to decay as $\rho(t) \sim t^{-\delta}$ with the DI critical exponent $\delta \simeq 0.285$ [21]. Figure 1 locates the critical point at $p_c = 0.510\,35(5)$, which is more accurate than that obtained in Ref. [32].

The IM is a lattice model with two possible states at each lattice point: either vacant or occupied by a particle. The dynamics begins with the adsorption attempt at a randomly selected vacant site. When both of the nearest neighbor (NN) sites are vacant, a monomer is adsorbed with rate 1. In case only one of the NN sites is occupied, the monomer is adsorbed on the substrate with rate λ, then reacts and leaves the substrate with the neighboring particle $(A+A \to \emptyset)$ instantaneously. When both NN sites are already occupied, the adsorption attempt is rejected. The dynamics on the substrate can be summarized as

$$VVV \xrightarrow{1} VAV, \tag{2a}$$

$$\left.\begin{array}{c} AVV \\ VVA \end{array}\right\} \xrightarrow{\lambda} VVV, \tag{2b}$$
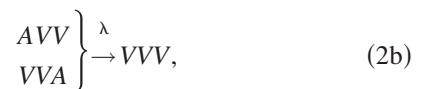
where A (V) means the monomer occupied (vacant) site.

The absorbing states of the IM are characterized by the "antiferromagnetically ordered" state $(\cdots AV\,AV\,AV\cdots)$ and have the Z_2 symmetry (poisoning even or odd sites by monomers). Starting with initial configurations without any AA pair, the proper order parameter ρ is the density of VV pairs.

The mapping of the dynamics of the IM to that of the contact process with the modulo 2 conservation [CP(2)] [36] is possible, though there are some subtleties which make these two models a little bit different. If we assign a domain wall excitation, say X, in the middle of the VV pair, the domain wall dynamics is exactly the same as the CP(2) rules. A pair annihilation in the CP(2) corresponds to an adsorption process of a monomer as in Eq. (2a) and a pair branching in the CP(2) to an annihilation process, Eq. (2b). Note that the reaction (2b) always generates two domain walls (two VV pairs), because an AA pair is not allowed in the IM. How-
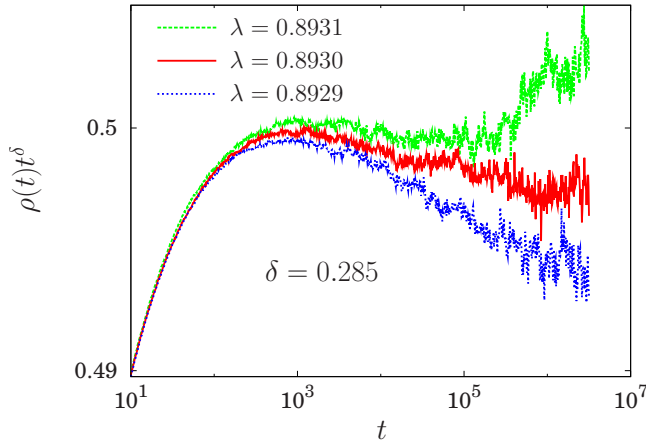
FIG. 2. (Color online) Semilogarithmic plots of $\rho(t)t^{\delta}$ vs t for the IM at $\lambda=0.8929$, 0.8930, and 0.8931 from bottom to top. The critical point is found to be $\lambda_c=0.8930(1)$.

ever, there is no one-to-one correspondence between configurations of the CP(2) and the IM, in general. For example, a domain wall configuration $X\emptyset X$ is not possible in the IM by definition, but is possible in the CP(2) in principle. Nevertheless, if we start with the fully occupied domain wall state, such a configuration cannot be generated by dynamics and thus the mapping becomes exact. In this case, the parameter q in Ref. [36] for the CP(2) is related to $1/(1+2\lambda)$ of the IM with suitable time rescaling. This mapping guarantees that the IM should belong to the DI class, which is confirmed by Fig. 2. We found the critical point of the IM to be λ_c $=0.8930(1)$ and, correspondingly, the more accurate critical point of the CP(2) as $q_c=0.358\,94(3)$ than that in Ref. [36].

III. THREE ROUTES TO THE DP CLASS

To study the crossover from the DI class to the DP class, we introduce dynamics with rate w which breaks either the symmetry or the mod-2 conservation. The crossover scaling ansatz of the order parameter at criticality is [15,34]

$$\rho(t;\Delta,w) = t^{-\delta}F(\Delta^{\nu_{\parallel}}t,w^{\mu_{\parallel}}t),\qquad(3)$$

where Δ is the deviation of a tuning parameter from the DI critical point. The meaning of Δ and w will be made clearer in the context of each crossover model. When $w=0$, the scaling function in Eq. (3) should describe the DI critical behavior. Hence, δ and $\nu_{\parallel}$ are the critical exponents of the DI classes: $\delta\simeq0.285$ and $\nu_{\parallel}\simeq3.2$, respectively [21]. The crossover exponent is defined as $\phi=\nu_{\parallel}/\mu_{\parallel}$, which can be measured from observing how the phase boundary behaves near the DI critical point

$$1/\phi = \lim_{w\to0^+} \frac{\ln\Delta_c(w)}{\ln w},\qquad(4)$$

where $\Delta_c(w)$ is the distance from the DI critical point at w $=0$ to the DP critical point at nonzero w.

First, consider the conservation-breaking (CB) route by introducing the mod-2 conservation breaking dynamics to the BAW2. When a particle tries to branch offspring, the

number of offspring is 2 (1) with the probability $1-w$ (w). This crossover model with finite w will be referred to as the BAWCB.

Second, the SB route is constructed by introducing the symmetry-breaking dynamics to the IM in such a way that the adsorption rate Eq. (2) at even-indexed sites is different from that of odd-indexed sites. To be specific, we modify adsorption dynamics without affecting the desorption events as

$$VV_{\mathrm{o}}V \xrightarrow{1-w} VA_{\mathrm{o}}V, \quad VV_{\mathrm{e}}V \xrightarrow{1} VA_{\mathrm{e}}V,\qquad(2a')$$

where the subscripts o and e refer to odd- and even-indexed sites, respectively. When $0<w<1$, this system prefers the absorbing state of poisoning monomers at even-indexed sites, which breaks the Z_2 symmetry of the IM. We will refer to the model with dynamics Eqs. (2a′) and (2b) as the IMSB.

Finally, the CC route can be constructed by connecting two equivalent symmetric absorbing states through infinitely many absorbing configurations [5]. In the context of the IM model, this route can be studied by allowing an adsorption without a pair reaction probabilistically as follows:

$$AVV \xrightarrow{w} AAV, \quad VVA \xrightarrow{w} VAA.\qquad(2c)$$
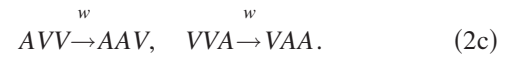
The model with dynamics of Eqs. (2a)–(2c) will be called the IMCC. As an adsorption attempt at a vacant site between two monomers (AVA) is still rejected, any configuration without a VV pair is absorbing and the order parameter is still the VV pair density. In contrast to the IM, the IMCC has infinitely many absorbing states characterized by the AA pair density (auxiliary field density). By pasting the two antiferromagnetically ordered absorbing states, we find either $\ldots VAV\,AAV\,AV\ldots$, which is already absorbing, or $\ldots VAV\,AVV\,AV\,AV\ldots$, which can evolve back to an absorbing state by adsorbing a monomer at either site of the VV pair. Hence there is no infinite dynamic barrier between absorbing states and the system leaves the DI class into the DP class.

Now we are equipped with three different models which can show the crossover behavior from the DI class to the DP class. As explained above, the crossover exponent ϕ can be deduced from the DP phase boundary near the DI critical point [see Eq. (4)]. For each model, the critical points at finite w are located numerically using the DP values of the critical exponents (see Table I). The critical points for the IMSB and IMCC are denoted by $\lambda_c(w)$ and for the BAWCB by $p_c(w)$, respectively. To measure the crossover exponent, we define $\Delta_c(w)\equiv|\lambda_c(w)-\lambda_c(0)|/\lambda_c(0)$ for the IMSB and the IMCC, and similarly $\Delta_c(w)\equiv|p_c(w)-p_c(0)|/p_c(0)$ for the BAWCB.

In Fig. 3, the crossover exponents are estimated for all three different routes. Along the SB route, we estimate ϕ $=2.1(1)$, which is consistent with previous estimates: ϕ $=2.1(1)$ [29], 2.24(10) [31], and recently, 1.9(1) [37]. Along the CB route, our estimate is $\phi=4.6(2)$, which is close to the recent result $\phi=4.8(2)$ [37]. Along the CC route, we find $\phi=2.9(1)$, which is clearly different from those for the SB and CB routes.

TABLE I. Critical point values $\lambda_c(w)$ of the IMSB and IMCC and $p_c(w)$ of the BAWCB for various w's. The numbers in parentheses indicate the uncertainty of the last digits.

w	$\lambda_c(w; \text{IMSB})$	$\lambda_c(w; \text{IMCC})$	$p_c(w; \text{BAWCB})$
0	0.8930(1)	0.8930(1)	0.510 35(5)
10^{-5}		0.9119(1)	0.4931(1)
2×10^{-5}			0.490 30(5)
5×10^{-5}		0.925 45(5)	0.4858(1)
10^{-4}		0.9340(1)	0.481 65(5)
2×10^{-4}		0.944 95(5)	0.4767(1)
3×10^{-4}			0.473 45(5)
5×10^{-4}	0.9125(2)	0.965 35(5)	0.468 90(5)
10^{-3}	0.9199(1)	0.9842(1)	0.461 75(5)
2×10^{-3}	0.9303(2)		
4×10^{-3}	0.944 75(5)		

IV. CROSSOVER MECHANISM

We found the three different routes for the crossover from the DI to the DP class, which yield all three different crossover exponents. It indicates that the crossover operator associated with each route should be different from each other. The difference between the SB and CB routes has been noticed earlier [22]. Summarizing it in the domain-wall (particle) representation, the crossover operator in the CB route is a single particle annihilation or creation operator in the action, while that in the SB route is a nonlocal string operator (global product of particle number operators) [22]. Hence it is not surprising to find that the two crossover exponents are different.

The crossover behavior along the CC route is tricky. First, note that the Z_2 symmetry between the odd-indexed and even-indexed sites is not broken in this route, which implies that the CC route is different from the SB one. Second, in
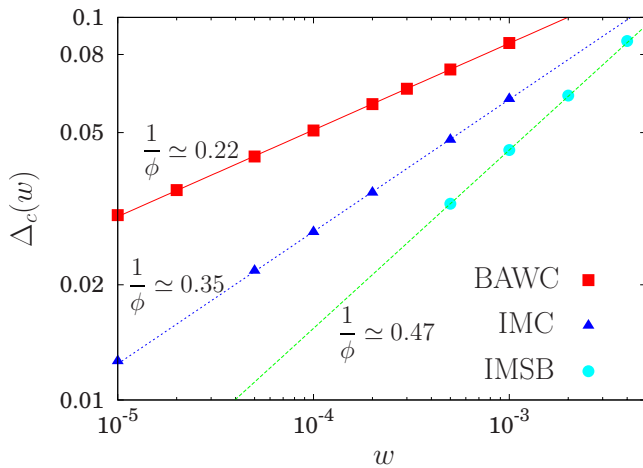

FIG. 3. (Color online) Log-log plot of $\Delta_c(w)$ vs w for three different crossover models. For graphical clarity, we shifted the y axis with arbitrary scale. The numerical values on the y axis are only for a guide to the readers. Each line whose slope is $1/\phi$ shows the fitting result for the corresponding phase boundary.
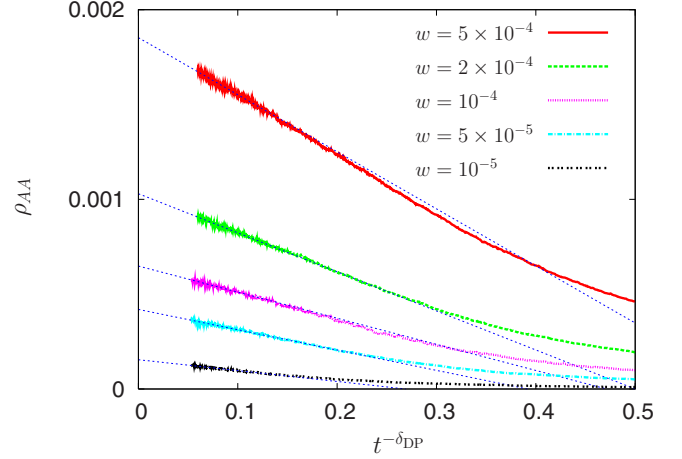

FIG. 4. (Color online) Long-time behavior of the auxiliary field density ρ_{AA} for small w's for the IMCC. The exponent $\delta_{\text{DP}} \simeq 0.160$ is the temporal decay exponent of the order parameter in the DP class. Simple extrapolation lines are given by dotted lines.

terms of domain walls, the CC process, Eq. (2c), clearly breaks the mod-2 conservation in the number of VV pairs (primary field X), because of which one may naively guess the CB-type crossover along the CC route. However, unlike the ordinary CB models, the CC process generates an infinite number of absorbing configurations with AA pairs (auxiliary field Y), which affect the domain wall (X) dynamics.

Consider the dynamics of the IMCC in terms of two fields X and Y. The reactions, Eqs. (2a) and (2b), can be rewritten as $2X \rightarrow \emptyset$ and $X \rightarrow 3X$, while Eq. (2c) is equivalent to $X \rightarrow Y$. The presence of AA pairs allows another reaction of $XY \rightarrow 2X$ ($AVV\,AA \rightarrow AVVV\,A$) in combination with Eq. (2b). The last two reactions involving the auxiliary field represent the feedback which generates memory effects on the primary field.

A. Auxiliary field density

The emergence of the auxiliary field density and the feedback mechanism may be responsible for the new crossover behavior along the CC route. To see how the auxiliary field may affect the crossover, we measure the auxiliary field density (natural density) $\rho_{AA}(w)$ along the DP critical line for the IMCC model.

We expect its long-time temporal behavior as $\rho_{AA}(w,t) = \rho_{AA}(w) - bt^{-\delta_{\text{DP}}}$ starting from the A particle vacuum [7,38], where δ_{DP} is the temporal decay exponent of the order parameter in the DP class. Figure 4 confirms our expectation and the asymptotic values of ρ_{AA} are plotted against w in Fig. 5. It is clear that $\rho_{AA}(0) = 0$ at the DI critical point. Near $w = 0$, the power-law singularity is found as $\rho_{AA} \sim w^{\alpha}$, with $\alpha = 0.65(2)$. We test the universality of the CC crossover scaling as well as the singularity of the auxiliary field density by investigating various different models like a CC variant of the interacting monomer-dimer model [39] and a two-species particle model defined as below. It turns out that these models form one crossover universality class with the same CC-type crossover exponent ϕ and the auxiliary field density exponent α [39].
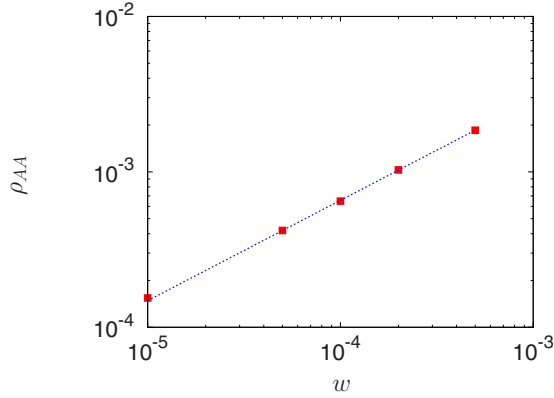
FIG. 5. (Color online) Log-log plot of ρ_{AA} in the steady state versus w for the IMCC. The slope of the dotted line is 0.645.

B. Memory effect

To examine the exclusive role of the feedback (memory) effect, we introduce a two-species (X, Y) particle model where the feedback process can be directly controlled. The primary particles X can diffuse, while the secondary particles Y are immobile. Each species' particles are hard core particles, but a simultaneous occupation by different species at a site is allowed. Therefore each site can be in one of four distinct states such as $\emptyset$, X, Y, and XY.

The reactions dynamics is symbolically summarized as $2X \rightarrow \emptyset$, $X \rightarrow 3X$, $X \rightarrow Y$, and $XY \rightarrow Y$, $2X$, or $3X$. To be more specific, the evolution rule is given as follows: First, choose one of X particles randomly. With probability w, the chosen X spontaneously mutates or annihilates as $X \rightarrow Y$ or $XY \rightarrow Y$. With probability $p - w$, the X hops to one of its neighboring sites. Whenever two X particles attempt to occupy the same site, they annihilate immediately like in the BAW2. With probability $1 - p$, the X can branch particles in the neighborhood as $X \rightarrow X + 2X$ with the dynamic branching rule [32]. To control the feedback effect, we introduce a parameter r in the branching process when a Y resides along with the chosen X at the same site, such that $XY \rightarrow X + 2X$ with the relative rate $(1-r)$ and $XY \rightarrow X + X$ with r.

At $w=0$, there is no spontaneous annihilation (or mutation) process and the model becomes exactly the same as the BAW2 (DI class) after some transient period needed for removing all Y particles via branching processes. At finite w, we expect the DP scaling with a finite density of Y particles; $\rho_Y(w) > 0$ because X particles generate Y particles via mutation processes, which cannot be fully eliminated via branching processes. So the CC-type crossover from the DI to the DP is expected, in general, as w becomes nonzero.

However, the $r=0$ point is special. There, the presence of Y particles never affects the dynamics of X particles, so there is no feedback mechanism to alter the primary particle density through the secondary particles. The primary field dynamics is basically identical to the BAWCB model introduced in Sec. III and the CB-type crossover scaling should appear at $r=0$ along with nonzero $\rho_Y(w)$. At finite r, the X particle dynamics is affected by the presence of Y particles, which generates the memory effects on the X particle density. Hence r can be regarded as the feedback controlling parameter and w as the crossover parameter.
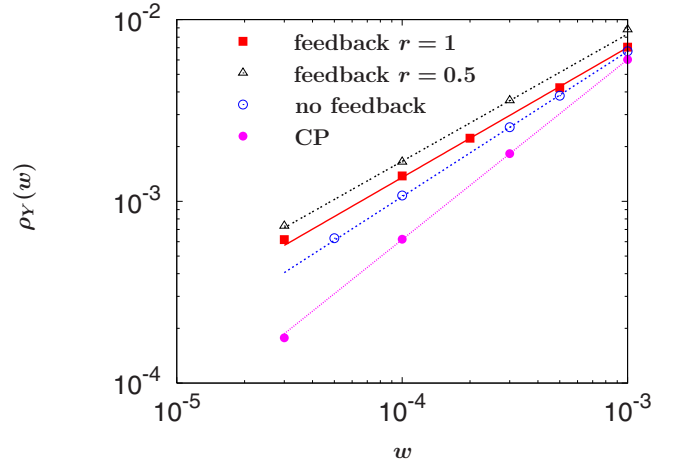

FIG. 6. (Color online) $\rho_Y(w)$ vs w along the phase boundary for the two-species model with ($r=1$ and 0.5) or without ($r=0$) feedback processes as well as the variant of the contact process (see the text) in double logarithmic scales. The slopes of the straight lines are 0.70, 0.71, 0.80, and 1 from above.

We performed numerical simulations for various values of r. For nonzero r, we found that the secondary particle density behaves as $\rho_Y(w) \sim w^\alpha$, with $\alpha = 0.70(3)$ and the crossover exponent $\phi = 3.1(2)$, both of which are consistent with the CC crossover results for the IMCC model within numerical errors. In contrast, at $r=0$, the CB crossover ($\phi \approx 4.6$) is found as expected along with $\alpha \simeq 0.80$ different from the CC crossover case (see Fig. 6). This leads to the conclusion that the feedback process, or equivalently memory, is crucial in establishing the CC-type crossover universality class and affects the singularity characteristic of the auxiliary field density.

It is interesting to note that the numerical values of α suggest a simple conjecture that $\alpha = 1 - 1/\phi$ for the DI to the DP crossover with an emerging auxiliary field. The mean field analysis leads to $\alpha=0$ and $\phi=1$ (see Appendix), which is also consistent with this conjecture. This implies that the nontrivial singularity in ρ_Y is directly related to the nontrivial crossover from the DI to the DP. Then, it is natural to ask what will happen if there is no nontrivial crossover. To answer this question, we study a two-species version of the contact process (CP) with the secondary particles: $X \rightarrow \emptyset$, $X \rightarrow 2X$, $X \rightarrow Y$, and $XY \rightarrow Y$, X, or $2X$ with the crossover parameter w controlling the $X \rightarrow Y$ process and the feedback parameter r controlling the $XY \rightarrow X$. This model belongs to the DP class for any value of w and r, including $w=0$. Therefore there is no "true" crossover in this model. We found the trivial linear phase boundary $[\Delta_c(w) \sim w]$ as expected and also the trivial behavior of ρ_Y with $\alpha=1$ regardless of the presence of the feedback processes (see Fig. 6). These results are consistent with the mean field results described in the Appendix.

C. DI models with finite auxiliary field density

Up to now, we have only been interested in the emergence of the auxiliary field for a finite crossover parameter w along

the CC route. One may consider more general cases where the auxiliary field density ρ_Y is finite (infinitely many absorbing states) even at the DI critical point ($w=0$). First, we studied the crossover behavior to the DP models with a continuous variation of ρ_Y as w increases. We found that $\rho_Y(w) - \rho_Y(0) \sim w^{0.22}$ and the crossover scaling belongs to the CB class [39]. This implies that the vanishing ρ_Y (not just singularity near $w=0$) is another important ingredient in the CC crossover. Note that $\rho_Y(w)$ seems to behave in the same way as the phase boundary $\Delta_c(w) \sim w^{1/\phi}$ with $1/\phi \simeq 0.22$ for the CB crossover.

Second, there may be a discontinuous drop in ρ_Y in the crossover to the DP with a single absorbing state ($\rho_Y=0$). This case may be compared to our previous study on the crossover from the DP with finite ρ_Y to the DP with $\rho_Y=0$ and similarly from the DI with finite ρ_Y to the DI with $\rho_Y =0$ [35]. As understood in Ref. [35], this crossover may be characterized by a discontinuous jump in the phase boundary at the DI critical point for the excitatory route or a continuous phase boundary for the inhibitory route. Along the inhibitory route in our case, where the DI with finite ρ_Y crosses over to the DP with $\rho_Y=0$, the CB crossover is observed again (not shown here) and we conclude that the discontinuity in the auxiliary field density does not provide any new crossover scaling [39].

V. SUMMARY

We studied three routes of the crossover from the DI to the DP class: SB, CB, and CC routes. These three routes are characterized by three different crossover exponents. The difference between the SB route and the CB route is clear because the symmetry-breaking field can be interpreted as the spatial nonlocal operator affecting the domain wall dynamics, while the conservation breaking corresponds to the local operator. The CB route and the CC route share some common features, but the feedback memory effect (or temporal nonlocality) makes the CC crossover distinct from the CB crossover. We also found the universal exponent $\alpha =0.65(2)$, which describes the singularity of the vanishing auxiliary field in the CC route. From the numerical study of the feedback controlling model and its mean field theory, we conjectured that $\alpha=1-1/\phi$.

APPENDIX: MEAN FIELD THEORY

This appendix provides the mean field theory for the feedback controlling model introduced in Sec. IV. Here ρ_X and ρ_Y are the densities of X and Y particles, respectively, and ρ_Z is the density of sites where both X and Y particles reside. Then one may easily write down the mean field equations as

$$\frac{\dot{\rho}_X}{\rho_X} = 2q - w - 2(1+q-w)\rho_X - rq\left(\frac{\rho_Z}{\rho_X} - 2\rho_Z\right), \quad (A1)$$

$$\dot{\rho}_Y = w\rho_X - (q+w)\rho_Z, \quad (A2)$$

$$\frac{\dot{\rho}_Z}{\rho_Z} = -1 + (\rho_Y - 2\rho_Z)\left[(1+q-w)\frac{\rho_X}{\rho_Z} - rq\right], \quad (A3)$$

where $q \equiv 1-p$. Since $p_c(w=0)=1$ in the mean field theory, q is the same as Δ in the text.

In the active phase, the steady-state density can be calculated by setting $\dot{\rho}_X=0$ and so on. The superscript s in the following indicates the steady-state density. From Eq. (A2), we get in the active phase

$$\frac{\rho_X^s}{\rho_Z^s} = 1 + \frac{q}{w}. \quad (A4)$$

Hence Eq. (A3) gives the steady-state density of ρ_Y^s such that

$$\rho_Y^s = 2\rho_Z^s + \frac{1}{(1+q-w)\rho_X^s/\rho_Z^s - rq}$$

$$= 2\rho_Z^s + \frac{w}{q(1-wr+q) + w(1-w)}. \quad (A5)$$

In the active phase, the (stable) steady-state density ρ_Y^s is determined uniquely, so we define the natural density at criticality by taking the limiting process from the active side as $\lim_{q \to q_c^+} \rho_Y^s(q)$. From Eqs. (A1) and (A4), the critical point is determined by the equation $-rq+(2q-w)(1+q/w)=0$, which reads

$$q_c = \frac{w}{4}\{\sqrt{8 + (1-r)^2} - (1-r)\}. \quad (A6)$$

For any value of $r(\leq 1)$, $q_c \sim \Delta_c \sim w$, which gives $\phi=1$. Since $\rho_Z^s=0$ at criticality, we get $\rho_Y^s \sim w/q_c \sim w^0$ from Eq. (A5), yielding $\alpha=0$. In low dimensions, q_c is expected to renormalize such that $q_c \sim \Delta_c \sim w^{1/\phi}$, which leads to the conjecture $\alpha=1-1/\phi$.

For comparison, we study the two-species version of the contact process with the secondary particles introduced in Sec. IV. The mean field equations are

$$\dot{\rho}_X = (2q-1)\rho_X - q\rho_X^2 - rq\rho_Z(1-\rho_X), \quad (A7)$$

$$\dot{\rho}_Y = w\rho_X - (q+w)\rho_Z, \quad (A8)$$

$$\dot{\rho}_Z = -\rho_Z + q(\rho_Y - \rho_Z)(\rho_X - r\rho_Z), \quad (A9)$$

where $q=1-p$. Then one may easily show that the critical line and the critical steady-state density of Y particles are given as for small w,

$$\Delta_c \simeq \frac{r}{2} w,$$

$$\rho_Y^s = \frac{w}{q_c^2 + q_c(1 - r)w} \simeq 4w, \qquad \text{(A10)}$$

where $\Delta_c = q_c(w) - 1/2$. As expected, we find the trivial linear phase boundary and also the trivial value of $\alpha = 1$, which is consistent with the simulation results shown in Fig. 6. Moreover, the renormalization cannot generate a singular behavior in the denominator of Eq. (A10), so α is always expected to be 1 in all dimensions.

[1] H. Hinrichsen, Adv. Phys. **49**, 815 (2000); G. Ódor, Rev. Mod. Phys. **76**, 663 (2004).

[2] H. K. Janssen, Z. Phys. B: Condens. Matter **42**, 151 (1981).

[3] P. Grassberger, Z. Phys. B: Condens. Matter **47**, 365 (1982).

[4] G. Grinstein, Z.-W. Lai, and D. A. Browne, Phys. Rev. A **40**, 4820 (1989).

[5] W. M. Hwang and H. Park, Phys. Rev. E **59**, 4683 (1999).

[6] M. C. Marques and J. F. F. Mendes, Eur. Phys. J. B **12**, 123 (1999).

[7] H. S. Park and H. Park, J. Korean Phys. Soc. **38**, 494 (2001).

[8] I. Jensen, Phys. Rev. Lett. **70**, 1465 (1993).

[9] A. Jiménez-Dalmaroni and H. Hinrichsen, Phys. Rev. E **68**, 036103 (2003).

[10] For a review, see M. Henkel and H. Hinrichsen, J. Phys. A **37**, R117 (2004).

[11] J. Kockelkoren and H. Chaté, Phys. Rev. Lett. **90**, 125701 (2003).

[12] J. D. Noh and H. Park, Phys. Rev. E **69**, 016122 (2004).

[13] S.-C. Park and H. Park, Phys. Rev. Lett. **94**, 065701 (2005); Phys. Rev. E **71**, 016137 (2005).

[14] H. Hinrichsen, Physica A **361**, 457 (2006).

[15] S.-C. Park and H. Park, Phys. Rev. E **73**, 025105(R) (2006).

[16] H.-K. Janssen, F. van Wijland, O. Deloubriere, and U. C. Täuber, Phys. Rev. E **70**, 056114 (2004).

[17] P. Grassberger, F. Krause, and T. von der Twer, J. Phys. A **17**, L105 (1984); P. Grassberger, *ibid.* **22**, L1103 (1989).

[18] H. Takayasu and A. Yu. Tretyakov, Phys. Rev. Lett. **68**, 3060 (1992).

[19] M. H. Kim and H. Park, Phys. Rev. Lett. **73**, 2579 (1994); H. Park, M. H. Kim, and H. Park, Phys. Rev. E **52**, 5664 (1995).

[20] N. Menyhárd, J. Phys. A **27**, 6139 (1994).

[21] I. Jensen, Phys. Rev. E **50**, 3623 (1994).

[22] W. M. Hwang, S. Kwon, H. Park, and H. Park, Phys. Rev. E **57**, 6438 (1998).

[23] J. D. Noh, H. Park, and M. den Nijs, Phys. Rev. E **59**, 194 (1999).

[24] O. Al Hammal, H. Chaté, I. Dornic, and M. A. Muñoz, Phys. Rev. Lett. **94**, 230601 (2005).

[25] S.-C. Park and H. Park, Eur. Phys. J. B **64**, 415 (2008).

[26] K. Park, H. Hinrichsen, and I.-M. Kim, Phys. Rev. E **63**, 065103(R) (2001).

[27] H. Park and H. Park, Physica A **221**, 97 (1995).

[28] N. Menyhárd and G. Ódor, J. Phys. A **29**, 7739 (1996).

[29] K. E. Bassler and D. A. Browne, Phys. Rev. Lett. **77**, 4094 (1996); Phys. Rev. E **55**, 5225 (1997).

[30] H. Hinrichsen, Phys. Rev. E **55**, 219 (1997).

[31] S. Kwon, W. M. Hwang, and H. Park, Phys. Rev. E **59**, 4949 (1999).

[32] S. Kwon and H. Park, Phys. Rev. E **52**, 5955 (1995).

[33] J. L. Cardy and U. C. Täuber, Phys. Rev. Lett. **77**, 4780 (1996); J. Stat. Phys. **90**, 1 (1998).

[34] See, e.g., I. D. Lawrie and S. Sarbach, in *Phase Transitions and Critical Phenomena*, edited by C. Domb and J. L. Lebowitz (Academic Press, London, 1984), Vol. 9.

[35] S.-C. Park and H. Park, Phys. Rev. E **76**, 051123 (2007).

[36] N. Inui and A. Yu. Tretyakov, Phys. Rev. Lett. **80**, 5148 (1998).

[37] G. Ódor and N. Menyhárd, Phys. Rev. E **78**, 041112 (2008).

[38] G. Ódor, J. F. F. Mendes, M. A. Santos, and M. C. Marques, Phys. Rev. E **58**, 7020 (1998).

[39] S.-C. Park and H. Park (unpublished).